**McCoy-West, Alex J., Davis, Alison M., Wainwright, Ashlea N., and Tomkins, Andrew G. (2024)** ***Simplifying silver isotope analysis of metallic samples: using silver nitrate precipitation to avoid perilous chloride formation.*** **Journal of Analytical Atomic Spectrometry, 39 (3) pp. 780-790.**

https://doi.org/10.1039/d3ja00374d

Check for updates

View Article Online
View Journal

# JAAS

Journal of Analytical Atomic Spectrometry

## Accepted Manuscript

This article can be cited before page numbers have been issued, to do this please use: A. J. McCoy-West, A. M. Davis, A. N. Wainwright and A. G. Tomkins, *J. Anal. At. Spectrom.*, 2024, DOI: 10.1039/D3JA00374D.

Volume 32
Number 1
January 2017
Pages 1-202

JAAS
Journal of Analytical Atomic Spectrometry
rsc.li/jaas

ISSN 0267-9577

ROYAL SOCIETY OF CHEMISTRY

PAPER
José-Luis Todolí *et al.*
Analysis of whole blood by ICP-MS equipped with a high temparature total sample consumption system

This is an Accepted Manuscript, which has been through the Royal Society of Chemistry peer review process and has been accepted for publication.

Accepted Manuscripts are published online shortly after acceptance, before technical editing, formatting and proof reading. Using this free service, authors can make their results available to the community, in citable form, before we publish the edited article. We will replace this Accepted Manuscript with the edited and formatted Advance Article as soon as it is available.

You can find more information about Accepted Manuscripts in the Information for Authors.

Please note that technical editing may introduce minor changes to the text and/or graphics, which may alter content. The journal's standard Terms & Conditions and the Ethical guidelines still apply. In no event shall the Royal Society of Chemistry be held responsible for any errors or omissions in this Accepted Manuscript or any consequences arising from the use of any information it contains.

ROYAL SOCIETY OF CHEMISTRY

rsc.li/jaas

View Article Online
DOI: 10.1039/D3JA00374D

ARTICLE

# Simplifying silver isotope analysis of metallic samples: Using silver nitrate precipitation to avoid perilous chloride formation

Received 00th January 20xx,
Accepted 00th January 20xx

DOI: 10.1039/x0xx00000x

Alex J. McCoy-West[a,b,c]*, Alison M. Davis[b], Ashlea N. Wainwright[d,b], Andrew G. Tomkins[b]

Silver (Ag) isotopes have the potential to provide useful insights into a diverse range of geological, environmental, and archaeological processes. This manuscript presents a novel technique that provides a simple, time-efficient, and accurate method for obtaining Ag isotope compositions of metallic gold (Au) samples. Unlike previous methodologies that favoured multiple ion exchange columns to purify and isolate Ag in nitrate form. This technique instead uses a single anion-exchange column, followed by the chemical conversion of Ag from chloride to nitrate form using the widely available reagents, ammonium hydroxide and ascorbic acid. This chemical conversion not only speeds up and simplifies sample processing allowing increased sample throughput, but importantly also significantly reduces the risk of Ag loss (and therefore user-induced isotopic fractionation) while converting the samples into a medium suitable for mass spectrometry. In this study, both pure Ag and native Au samples have been investigated, with Ag isotope compositions given relative the NIST SRM978a Ag standard. The long-term reproducibility of the in-house Sigma MON Ag solution was $\varepsilon^{109}$Ag = 1.32 ± 0.31 (2 s.d.; n = 34), which is comparable to the precision achievable for unprocessed high-purity Ag samples with replicate analyses generating an average precision of $\varepsilon^{109}$Ag = ± 0.25 (2 s.d.; n = 5). Comparable levels of precision were also achieved for natural Au samples, indicating that this methodology has no resolvable effect on the precision of the Ag isotope measurements. The natural Au standard CEZAg was used to test the external reproducibility of the chemical separation and conversion technique, yielding an average value of $\varepsilon^{109}$Ag = 0.34 ± 0.13 (2 s.d.; n = 6), which is within analytical uncertainty of the previous determinations, demonstrating the accuracy of the new methodology. Furthermore, analysis of natural Au gold nuggets from the Fosterville Au Mine using the chemical conversion process described herein and a previously published multiple column method at a different institution produced consistent Ag isotope compositions, confirming the accuracy of the measurements generated using this method.

## 1. Introduction

Silver (Ag; Z = 47) isotope geochemistry has undergone a renaissance in popularity in recent years due to the widespread availability of multi-collector induction coupled plasma mass spectrometers (MC-ICP-MS) and its potential applications in geoscience [1-7], archaeology [8-13], and environmental science [14, 15]. Prior to the advent of MC-ICP-MS technology, Ag isotope measurements were carried out using a thermal ionisation mass spectrometer (TIMS) with a precision of only ca. 1 – 2 ‰ achievable [16, 17]. This meant that only very large isotopic shifts of > 1% in $^{107}$Ag/$^{109}$Ag could be resolved, as seen in iron meteorites, where the radiogenic decay of primordial $^{107}$Pd to $^{107}$Ag with a half-life of just 6.5 ± 0.3 Ma was active [18]. As Pd is a more refractory and siderophile element than Ag, preferential fractionation of Pd from Ag into planetesimal cores early in the Solar System's history contributed to isotopically light signatures in early-formed iron meteorites (all thought to have formed within 5 Ma of the Sun, well before extinction of the radionuclide about 60 Ma after Solar System formation [7, 19]. More recent studies have taken advantage of the significant improvement in analytical precision available from multi-collector induction coupled plasma mass spectrometer (MC-ICP-MS) technology to measure the significantly smaller $^{107}$Ag/$^{109}$Ag shifts observed in terrestrial samples [2, 20, 21]. These mass-dependant Ag isotope fractionations (i.e. unrelated to $^{107}$Pd decay) are the result of physio-chemical processes and are reported in $\varepsilon^{109}$Ag (that is variations in $^{109}$Ag/$^{107}$Ag in parts per $10^4$) relative to the widely used reference material NIST SRM978a. Although Ag typically occurs in trace concentrations (5-70 ng/g) in its $Ag^+$ state in most rock types [21-24], in rare cases elevated concentrations of Ag can occur as native $Ag^0$ metal alloyed with gold (Au), antimony (Sb), tellurium (Te) or copper (Cu) or as $Ag^+$ in sulfide or sulfosalt ore minerals [25-27]. Therefore, the application of Ag isotope geochemistry to the field of economic geology is of particular interest [1, 3-6, 28-31]. These recent studies have investigated the use of Ag isotope ratios as an isotopic proxy for Au and to explain ore forming processes in Ag-bearing mineralised systems. Gold is mono-isotopic but is typically alloyed with a significant component of Ag (1-10 wt. %) when it occurs in native metallic form [6, 32]. As both metals have identical crystal structure and form $HS^-$ and $Cl^-$ complexes

---

[a] IsoTropics Geochemistry Laboratory, Earth and Environmental Sciences, James Cook University, Townsville, QLD 4811, Australia
[b] School of Earth, Atmosphere and Environment, Monash University, Clayton, Victoria, 3800, Australia
[c] Economic Geology Research Centre, James Cook University, Townsville, QLD 4811, Australia
[d] School of Geography, Earth and Atmospheric Sciences, University of Melbourne, Parkville, VIC 3010, Australia

Electronic Supplementary Information (ESI) available: Includes supplementary figures and tables. See DOI: 10.1039/x0xx00000x

View Article Online
DOI: 10.1039/D3JA00374D

during fluid transport, they are expected to have similar behaviours during ore forming processes [33]. Given the wide range of applications to economic geology, there is great incentive for developing a simple and reliable method for measuring the Ag-isotope composition of metallic Ag and Au samples.

The initial studies of Ag isotopes in silicate rocks and meteorites required three [2, 7, 19] or two [14, 21] step ion exchange procedures to efficiently separate Ag from a range of complex matrices. Multiple ion exchange columns are needed for whole rock samples due to the large variety of matrix elements and very low concentrations of Ag (<100 ng/g). While studies focusing on metallic ore samples (Ag = ca. 1-100 wt. %) have used none [1, 28], one [1, 3] or two [5, 6] columns for native Ag and Au samples depending on their purity. Brügmann et al. (2019) optimised previous methodologies to suit metallic Au samples creating a two-step ion exchange procedure: the first column was used to remove the matrix elements and the second was used to convert Ag from chloride form to nitrate form. This method [5] significantly speed up the first column, because Ag is not retained by the resin and elutes immediately and thus can be further processed more quickly compared to previous methods. In metallic Au samples, other than Au itself, ion exchange columns must also be effective at removing Cu (which can be present in concentrations up to ca. 1 wt.%) and Pd (which normally occurs at the ng/g level, but if not properly removed, will directly interfere during mass bias corrections). In this study, we present a new chemical conversion procedure to improve the methodology of Brügmann et al. (2019) to achieve an even faster separation process. Following the removal of matrix elements on an anion exchange column, Ag is then converted from its chloride to nitrate form using ammonium hydroxide and ascorbic acid. The entire process, from dissolution to samples being ready for mass spectrometry, can be completed in 1.5 days. This technique not only speeds up and simplifies sample processing, but also significantly reduces the risk of Ag loss (and therefore isotopic fractionation) while converting the samples into a medium suitable for mass spectrometry.

## 2. Experimental

### 2.1 Method outline

Silver-bearing metallic samples typically contain significant amounts of Au (e.g. native Au, electrum and historical coins) and require concentrated aqua regia ($HNO_3$ + 3HCl) for complete dissolution and will only remain stable in moderately concentrated solutions of hydrochloric acid (> 6M HCl). For this reason, initial ion exchange chromatography must be conducted in strong HCl media and therefore $Ag^+$ is eluted from the ion exchange columns in its chloride form. However, in order for the samples to be analysed using MC-ICP-MS, the Ag needs to be in nitrate form in a dilute solution of nitric acid ($HNO_3$). This is because $AgCl_{(s)}$ is highly insoluble in water and/or $HNO_3$, as the extremely low solubility product of AgCl in solution (Ksp = $10^{-10.48}$ ; [34]) limits the solubility of Ag in the presence of $Cl^-$ ions. Even trace amounts of $Cl^-$ ions in $AgNO_{3(aq)}$ rapidly causes the precipitation of insoluble $AgCl_{(s)}$,. Therefore, the main challenge of processing metallic Ag-bearing samples is to convert the $AgCl_{(aq)}$ solutions eluted from the columns into nitrate form and then keep $AgNO_{3(aq)}$ stable and in solution without re-contamination with $Cl^-$ ions (which can come from the atmosphere, for example). [5] reported a method that used a second ion exchange column filled with TBP (TriButyl-Phosphate) resin to convert Ag from chloride to nitrate form. Once the Ag-bearing solution is loaded on to the TBP column in HCl, the $Ag^+$ ions bond with the TBP resin until all $Cl^-$ ions are flushed out from the column, at which point $Ag^+$ can be eluted using $HNO_3$ [5].

Instead, the method presented here uses ammonium hydroxide ($NH_4OH$ or $NH_{3(aq)}$) to dissolve the $AgCl_{(s)}$ collected from the first ion exchange column and then ascorbic acid ($C_6H_8O_6$) to reduce the resulting $Ag^+$ ions into metallic Ag particles ($Ag^0$). Ascorbic acid is a reducing agent that is commonly used to remove cations, including $Ag^+$, from solutions by reducing them to their metallic form. Archaeological studies commonly use solvents to leach lead (Pb) and AgO from oxidised coins, which are then converted to an Ag-Pb nitrate solution, ascorbic acid can then be used to precipitate pure metallic Ag while leaving the Pb dissolved in the solution [8, 13]. Nano-particle technology studies have also used ascorbic acid in a similar manner to precipitate ultrafine Ag powder from $AgNO_{3(aq)}$ solutions [35, 36]. The method presented herein is based on those from the 1960's and 70's that used $NH_4OH$ and ascorbic acid to recover Ag metal from photographic materials and industrial waste containing AgCl e.g. [37]. It utilises the same reagents as part of a simple, reliable and high-yield method for purifying Ag from Au-bearing metallic samples and preparing the pure $AgNO_{3(aq)}$ solutions required for high precision analysis by MC-ICP-MS.

### 2.2 Reagents and materials

All wet chemistry was carried out in a class 350 clean laboratory in the Isotopia laboratories at Monash University. Concentrated HCl and $HNO_3$ were double distilled from reagent grade using a Savillex DST-4000 sub-boiling acid purification system. Reagent grade ascorbic acid and $NH_4OH$ were used due to the very small volumes used in sample processing. All water was deionised using the Milli Q system and produced a high purity (18.2 MΩ) water. Bio-Rad AG1-X8 (100-200 mesh $Cl^-$ form) ion exchange resin was acquired from Bio-Rad Laboratories (Hercules, California, USA). The resin was washed in MQ $H_2O$ and suspended particles were removed. All resin is single-use and disposed of after the ion exchange procedure. Disposable 0.5 mL Pasteur plastic pipettes were used as single-use ion-exchange columns. Columns were placed in a sealed 500 mL Teflon beaker filled with 2 % $HNO_3$ and placed on a hot plate at 60°C to clean for several days. Columns were then thoroughly rinsed with Milli Q water and dried prior to use. Frits were cut using a stainless steel cutting tool and made from Porex fine polyethylene sheet (XS-49000) with 20-60 μm pore size.

International reference materials for Ag NIST SRM978a and Pd NIST SRM3138 were obtained from National Institute of Standards and Technology (Gaithersburg, MD, USA). An in-house Ag standard was

View Article Online
DOI: 10.1039/D3JA00374D

developed using a Sigma-Aldrich 994 µg/mL Ag solution (Lot# BCBS0422V) and used for the purposes of method development and reproducibility testing. A Sigma-Aldrich 1000 µg/mL Au standard (Lot# BCBX4894) was also used for the purpose of method testing and development. Two synthetic Au-Ag standard mixtures were made for initial methodology testing by combining the two aforementioned Sigma-Aldrich Ag and Au solutions. These two synthetic standards Sigma5 and Sigma10 had 300 µg/mL Ag and 5700 µg/mL and 2700 µg/mL Au, respectively (replicating native Au samples with 5 and 10 wt.% Ag, respectively). Additionally, the natural Au-Ag nugget standard CEZAg was acquired from Curt-Engelhorn-Zentrum Archäometrie gGmbH, Mannheim, Germany (CEZ) this sample has previously been well characterised both chemically and isotopically [5, 6].

### 2.3 Sample selection and preparation

Natural samples (i.e. native Ag or Au) with visible inclusions or traces of other minerals (such as quartz or sulfides) should be avoided as this will cause issues during dissolution and significantly increase the abundance and variety of matrix elements in the sample. Due to the high malleability of Ag-Au alloys, the simplest way to ensure the sample doesn't contain unwanted inclusions is to use a clean flat surface (such as an agate pestle) to flatten the sample. Inclusions of non-metallic minerals will be crushed or powdered and can then be easily removed by rinsing flattened sample in Milli Q $H_2O$. For best results, samples should be examined under a microscope to ensure they are free from unwanted material and inclusions. Tarnished metallic Ag samples should also be avoided, as silver oxide (AgO) is insoluble in aqua regia or $HNO_3$. If analysis of partially oxidised samples is essential, then samples can be placed in $NH_4OH$ to dissolve the AgO, leaving metallic Ag undissolved [13].

Both natural Ag and Au samples have been analysed in this study. Four native Ag wire specimens from the Eleura Mine in Cobar, New South Wales, Australia, and an Ag coin from the Melbourne Mint, Australia (Fig. S1) were processed to access the data quality achievable for pure metallic Ag samples that have not been chemically processed. The native Ag wire (SW) specimens (SW01 – SW04) range in weight from 1.05 – 9.49 mg and have irregular elongated shapes, approximately 5 – 8 mm long and 1 – 2 mm in diameter (Fig. S2). These Ag wires have well-defined crystalline structures with multiple branches and minimal oxidation. Although these samples are high purity Ag, they may contain small amounts of matrix elements. Additionally, four native Au samples for the Fosterville Gold Mine in the Victorian Goldfields, Victoria, Australia were also analysed to test the reproducibility of the methodology presented herein. The samples comprise hand-sized pieces of quartz-carbonate vein material with stibnite and visible native Au mineralisation (Fig. S3). To further validate the methodology presented herein subsections of some of these samples were also analysed at the CEZ, Mannheim, Germany following the methodology of [5].

### 2.4 Sample digestion

Metallic Au samples were weighed and then dissolved in 7 mL Savillex PFA beaker using 1 mL of concentrated aqua regia (3 HCl : 1 $HNO_3$) and placed on a hotplate overnight at 80°C. If the sample was not fully dissolved after 24 hours, additional increments of 0.5 mL of aqua regia were added until complete dissolution was achieved. Following complete dissolution, sample solutions were dried down on a hotplate overnight at 80°C and the residue wasthen re-dissolved in 0.6 mL of 10 M HCl on the hotplate at 80°C for 2-3 hours and sonicated if required. These solutions were then diluted with 0.4 mL of MQ $H_2O$ to make final 1 mL solutions of 6 M HCl. Small aliquots (20 µL) were removed to determine the concentration of Ag in the solution using a ICP-MS. High purity metallic Ag samples (wires and coins) were weighed and then dissolved in a 7 mL Savillex PFA beakers using 1 mL of 8 M $HNO_3$ to form $AgNO_{3(aq)}$ solutions. Typically, samples dissolve in less than a few minutes without heating, but if required, samples can be placed on a hotplate overnight at 80°C. No further sample processing was required for the pure native Ag samples and the resulting $AgNO_{3(aq)}$ solutions can be diluted and directly used for MC-ICP-MS analysis.

### 2.5 Silver concentration via Q-ICP-MS

Silver concentrations in native Au samples can vary from 1 to 13 wt.% e.g. [1, 6], so it is important to determine the exact Ag concentration in the sample to avoid overloading columns during chromatographic separation. As mentioned above, a 20 µL aliquot of the sample solution was taken for measurement by quadrupole (Q)-ICP-MS prior to chromatographic separation. Samples were assumed to have a Ag concentration of 5 wt. % (95 wt. % Au) and the aliquot was diluted accordingly to an estimated 100 ng/mL Ag using 2 % $HNO_3$. Concentrations of Ag, Au, Cu and Pd in the sample aliquots were then determined using a Thermo-Fisher ICAP-Q Q-ICP-MS at Monash University. Calibration of the instrument was performed using mixed Sigma Aldrich solutions at specific concentrations (0.1 ng/mL, 1 ng/mL, 10 ng/mL, 100 ng/mL, 200 ng/mL). Throughout the session, the 100 ng/mL solution was re-analysed every 10 sample measurements to correct for any instrumental drift.

### 2.6 Chromatographic separation

Effective removal of matrix elements is essential for obtaining accurate and precise MC-ICP-MS measurements. Matrix elements can generate polyatomic interferences (i.e. $^{67}Zn + ^{40}Ar \approx ^{107}Ag$) during analyses, or in the case of Pd and Cd, could interfere with mass bias corrections creating spurious data. The initial chromatographic separation procedure used here for separating Au and Pd from Ag was presented in Brügmann et al. (2019). The effectiveness of this separation protocol was also verified herein with elution curves presented in Figure S4. This method is suitable for samples containing up to 300 µg of Ag, where the main matrix element is Au (up to ca. 99 % Au). If the sample was determined by Q-ICP-MS to have greater than 300 µg/mL Ag, it was then diluted with 6 M HCl so that a loading volume of 1 mL contains ≤ 300 µg of Ag. For Ag-poor samples with greater than 99 wt.% Au (< 1 wt.% Ag), further dilution is required to avoid the columns becoming physically overloaded with Au [5].

View Article Online
DOI: 10.1039/D3JA00374D

A summary of the ion exchange procedure is provided in Table 1. The use of anion exchange resin AG1-X8 (100-200 mesh $Cl^-$ form) provides an ideal medium for the separation of Au and Pd from Ag due to the large difference in elution behaviour when the elements are in HCl (Schönbächler and Fehr, 2013). Columns were made from disposable 0.5 mL Pasteur plastic pipettes with an internal diameter of 3 mm, cut to 45 mm in length (excluding the reservoir) (Fig. S5a). Frits made from porous polyethylene with 20-60 μm pore size were inserted 3 mm from the tip of the column. The columns were then filled with 0.3 mL (40 mm resin bed length) of AG1-X8 resin (100-200 mesh $Cl^-$ form). The resin was cleaned and preconditioned with 3 mL 6 M HCl (6 increments of 0.5 mL). The sample solution (1 mL of 6 M HCl) was then loaded onto the column. Silver begins to elute from the column immediately, while Au and Pd remain strongly bonded to the resin, therefore Ag collection begins immediately into acid leached 7 mL PFA Teflon beakers. A further 4 mL of 6 M HCl (8 increments of 0.5 mL) was then added to the column and collected into the same beaker. This 5 mL of elutant should contain >99 % of the Ag [5] from the sample while the Au and the Pd remain on the column and form a dark yellow/orange cap at the top of the column (Fig. S5c).

### 2.7 Conversion of Ag from chloride to nitrate form

Once matrix elements have been removed from the sample solution via ion exchange chromatography, the Ag needs to be converted from chloride ($AgCl_{(aq)}$) to nitrate form ($AgNO_{3(aq)}$) to proceed with mass spectrometry. In the method presented here, this conversion is achieved without the need for an additional ion exchange column (Fig. 1). The 5 mL of 6 M HCl eluted from the columns is evaporated on a hotplate in the PFA Teflon beaker until the volume has reduced to ≤ 1.5 mL. Care must be taken that complete evaporation does not occur during this step, hence a moderate temperature is preferable. This reduced volume of solution was then transferred to a 1.5 mL polypropylene centrifuge tube and dried down on a hotplate at a maximum of 60°C overnight to form a white precipitate of $AgCl_{(s)}$. At this point, care should be taken (i.e. procced with the following steps as soon as practical) to minimise exposure of the $AgCl_{(s)}$ to light (especially ultraviolet), as it is highly photo-sensitive and will begin to decompose into Ag metal and $Cl^-$ gas. Light mitigation measures taken include turning off any fume hood and room lights during the evaporation phase and storing any dry sample residues in opaque containers. Transferring samples to a centrifuge tube at this stage was found to be optimal, as it allows the volume of $NH_4OH_{(aq)}$ added to be minimised, and ensures that the reaction proceeds efficiently (i.e. avoids instances where the AgCl precipitates (via drying) onto the sides of the 7 mL beakers).

Using a Teflon drop-dispensing bottle, 2-3 drops (totalling approximately 200 μl) of 30 % $NH_4OH_{(aq)}$ is added to the precipitate of $AgCl_{(s)}$, which dissolves to form the aqueous diamminesilver (1) ion through the following reaction:

$$AgCl_{(s)} + 2NH_4OH_{(aq)} \rightarrow [Ag(NH_3)_2]^+_{(aq)} + Cl^-_{(aq)} + 2H_2O_{(l)}$$

The low viscosity and high vapour pressure of 30 % $NH_4OH_{(aq)}$ makes it difficult to accurately dispense using a Pasteur pipette, so a drop-dispensing bottle was found to be optimal. The precise volume of $NH_4OH_{(aq)}$ is not important, but should not exceed ca. 300 μl, to minimise potential contamination from the reagent grade $NH_4OH$

To aid the dissolution of the $AgCl_{(s)}$ the centrifuge vials are capped and placed on a vortex mixer for 30-60 seconds until all the $AgCl_{(s)}$ precipitate has dissolved. Since such a small volume of $NH_4OH_{(aq)}$ is used, agitating the solution allows any $AgCl_{(s)}$ that may be on the internal walls of the vial to come into contact with the solvent. Directly following dissolution of the $AgCl_{(s)}$, a 1 M ascorbic acid ($C_6H_8O_{6(aq)}$) solution is prepared. The ascorbic acid must be used immediately after preparation, as it begins to degrade within minutes. To each sample, 100 μL of 1 M ascorbic acid is added to the aqueous diamminesilver (1) solution and instantly micron-sized native Ag particles are formed (Fig. S6). The solution transitions from a clear colourless solution to a cloudy grey solution instantaneously. The ascorbic acid acts as a reducing agent and converts the $Ag^+$ in the diamminesilver (1) ion to its $Ag^0$ state via the following reaction:

$$2[Ag(NH_3)_2]^+_{(aq)} + C_6H_8O_{6\,(aq)} \rightarrow 2Ag_{(s)}\downarrow + C_6H_6O_{6\,(aq)} + 4NH_{3(aq)} + 2H^+_{(aq)}$$

The vial is then capped and agitated on a vortex mixer for 30 seconds to ensure the reactants are fully combined. This agitation also causes the suspended Ag particles to aggregate and settle to the bottom of the vial. The solution is then diluted to 1 mL with MQ $H_2O$ and centrifuged at 10,000 rpm for 5 minutes to ensure the Ag particles are separated from solution. The supernatant is then carefully removed using a pipette and placed into a storage beaker. The diluting, centrifuging and removal of the supernatant is repeated five times until the Ag particles are free from any traces of $NH_4OH_{(aq)}$ and ascorbic acid. The final supernatant is removed until all Ag particles in the bottom of the vial are contained in a small droplet of MQ $H_2O$ (Fig. S5b). The storage beaker containing all the removed supernatant can then be inspected to ensure it contains no $Ag^0$ particles.

The $Ag^0$ particles are then dissolved using 1 mL of 8 M $HNO_3$ to produce a solution of $AgNO_{3(aq)}$ (Fig. S7). Dissolution must be completed immediately after the conversion as the Ag particles begin to oxidise rapidly when exposed to air or MQ $H_2O$. This chemical conversion process has the additional benefit of removing any additional matrix elements that may have remained following the ion exchange chromatography. As Ag is the only cation that will precipitate during the reduction reaction, other elements (e.g. Pb) will remain in the supernatant and will therefore be discarded (e.g. Albarède et al., 2016; Desaulty et al., 2011). The entire chemical conversion process, from dry samples to purified $AgNO_{3(aq)}$ ready for dilution for the mass spectrometer, can be completed in 1-2 hours dependant on the number of samples.

### 2.8 Silver isotope measurements by MC-ICP-MS

Silver isotope measurements were determined using a Thermo Fisher Neptune Plus MC-ICP-MS at Monash University. A borosilicate

View Article Online
DOI: 10.1039/D3JA00374D

glass nebuliser (Glass Expansion MicroMist nebulizer) with a 50 µL/min uptake rate was used (Fig. S5d), as it was found to generate more reproducible isotope data than PFA nebulisers, during method optimisation. The PFA nebulisers were prone to drips forming near the tip, which led to additional signal instability. Samples are introduced into the factory-standard stable sample introduction (SSI) borosilicate glass dual cyclonic Scott spray chamber (Fig. S5d). All measurements were made in low resolution mode using an X skimmer cone, which produced a typical sensitivity of ca. 90 V/ppm Ag. Six isotopes were measured simultaneously during analysis $^{105}$Pd, $^{106}$Pd, $^{107}$Ag, $^{108}$Pd, $^{109}$Ag, $^{111}$ Cd, using the L2, L1, C, H1, H2 and H4 cups, respectively. A single analysis consisted of 1 block of 45 cycles of 4.2 second integrations with a typical analysis requiring ca. 25 ng of Ag. Washout times were 120 seconds, and measurements were immediately preceded by the analysis of an on-mass acid blank. An auto-sampler is used for sample introduction to ensure uptake and washout times are consistent throughout the analytical session. Standard operating conditions are reported in Table S1.

For analysis, sample solutions were diluted to 100 ng/mL Ag using 2 % $HNO_3$ on the day of the measurement. Given that Ag solubility is reduced once the sample is diluted, it is important that dilution is done as close to the time of analysis as practical. Once diluted, the signal intensity of each sample solution was recorded and compared to the signal intensity of the standard solution to determine the exact concentration of Ag. The Pd signal was also monitored at this stage, prior to doping, and should be at background intensities. This is most important for native Ag samples that have not undergone chemical processing. Palladium is used to correct for instrumental mass bias and all sample and standard solutions were doped using the NIST SRM3138 Pd standard, during this study $^{107}$Ag:$^{108}$Pd ratios ranged from 0.99-2.33, although an ideal ratio of 1:1 (ca. 190 ng/mL Pd) is recommended moving forward. Ion signals for $^{107}$Ag and $^{106}$Pd were consistently above 1 V (i.e. ≥ 2.6 V and 1.4 V, respectively), meaning that baseline effects and blank interference problems are insignificant. Although Ag has no direct isobaric interferences, the Pd isotopes $^{106}$Pd, $^{108}$Pd and $^{110}$Pd in low resolution have isobaric interferences with Cd isotopes $^{106}$Cd, $^{108}$Cd and $^{110}$Cd, respectively. The isobar free isotope $^{111}$Cd is monitored to access the amount of Cd, which can be used to undertake a Cd interference correction of the Pd signals during data processing. All isotopic measurements of Ag are reported in parts per 10,000 or standard epsilon ($\varepsilon$) notation, representing the difference in $^{109}$Ag/$^{107}$Ag relative to the NIST SRM978a, using the following equation:

$$\varepsilon^{109}\mathrm{Ag} = \left[\frac{\left(\frac{^{109}\mathrm{Ag}}{^{107}\mathrm{Ag}}\right)_{sample}}{\left(\frac{^{109}\mathrm{Ag}}{^{107}\mathrm{Ag}}\right)_{NIST\ SRM978a}}\right] \mathrm{x}\ 10{,}000$$

The international reference material NIST SRM978a was used as the primary bracketing standard and measured before and after every sample. The in-house Ag standard Sigma ICP was measured a minimum of three times at the beginning of each session and the isotopic offset from the NIST SRM978a was used to validate instrument performance. Most earlier studies reported Ag isotope ratios as $^{107}$Ag/$^{109}$Ag, as they were concerned with the large shifts in $^{107}$Ag in meteorite samples due to the decay of the short-lived radionuclide $^{107}$Pd (e.g. Schönbächler et al., 2008). Now that the focus of Ag isotope studies has begun to shift towards terrestrial samples, it is appropriate to report the isotopic ratio following stable isotope convention with the heavier isotope being the numerator ($^{109}$Ag/$^{107}$Ag). Uncertainties on individual measurements in diagrams are presented as propagated 2 s.e. and represent the uncertainty of the individual measurement (2 s.e.) added in quadrature to the average uncertainty (2 s.e.) of the corresponding bracketing NIST SRM978a measurements (complete data can be found in Electronic Supplementary Material).

Total procedural yields were calculated using $^{109}$Ag intensities determined during MC-ICP-MS measurements. Samples were diluted to 100 ng/mL based on the assumption that all 300 µg of Ag added to initial anion exchange column was retained throughout the entire protocol. Yields were then calculated relative to the average observed intensity of the bracketing standard diluted to the same concentration. Average Ag yields for Au dominated samples processed herein were 98.5 ± 10.1 % (2 s.d.; n = 11) and remain consistently high independent of the amount of Ag in the samples (Fig. S8). Given the large dilution factors and multiple dilution steps required for both ICP-MS and MC-ICP-MS measurements (assuming 5 wt.% Ag; 1:50,00,000 to 1:50,000, respectively), which all potentially introduce aliquoting errors, these results validate the quantitative Ag yield of the chemical conversion procedure described herein.

## 3. Results and discussion

Replicate measurements of synthetic standard solutions and Au reference materials are summarised in Table 2 and measurements of natural Ag and Au samples are summarised in Table 3.

### 3.1 Mass bias normalisation procedure

The use of an internal dopant of similar atomic mass to monitor instrumental mass bias during mass spectrometry is common practice and can help generate more reproducible isotopic ratios by minimizing the influence of minor matrix elements remaining in the solution and other analytical mismatches [15, 38-41]. For consistency with earlier Ag studies [1, 2, 5-7], we prefer to use $^{108}$Pd/$^{105}$Pd to calculate instrumental mass bias and generate mass-bias corrected $^{109}$Ag/$^{107}$Ag ratios. Instrumental mass bias ($\beta_{Pd}$) is calculated as follows:

$$\beta_{\mathrm{Pd}} = \ln\left[\frac{\left(\frac{^{108}\mathrm{Pd}}{^{105}\mathrm{Pd}}\right)_{measured}}{\left(\frac{^{108}\mathrm{Pd}}{^{105}\mathrm{Pd}}\right)_{reference}}\right] / \ln\left(\frac{M_{^{108}\mathrm{Pd}}}{M_{^{105}\mathrm{Pd}}}\right)$$

View Article Online
DOI: 10.1039/D3JA00374D

The Ag isotope composition corrected for instrumental mass fractionation ($^{109}Ag/^{107}Ag_{corrected}$) is then calculated:

$$\left(\frac{^{109}\mathrm{Ag}}{^{107}\mathrm{Ag}}\right)_{corrected} = \left(\frac{^{109}\mathrm{Ag}}{^{107}\mathrm{Ag}}\right)_{measured} \mathrm{x} \left(\frac{M_{^{109}\mathrm{Ag}}}{M_{^{107}\mathrm{Ag}}}\right)^{\beta_{\mathrm{Pd}}}$$

Given that Ag has only two stable isotopes, verifying the mass dependence of the isotope data is impossible. However, given that Pd has multiple isotopes, this normalisation procedure can be repeated using alternative Pd isotope ratios (i.e. $^{106}Pd/^{105}Pd$) to provide a secondary validation of data quality. The slopes of the linear regression lines for ln($^{108}Pd/^{105}Pd$) and ln($^{106}Pd/^{105}Pd$) versus ln($^{109}Ag/^{107}Ag$) generated using NIST SRM978a are shown in Figure 2. Most materials measured herein show excellent agreement with these mass fractionation lines, suggesting negligible matrix effects, although the Fosterville Au and native Ag wires do show a small mismatch, consistent with slightly different mass bias behaviour, probably due to trace matrix elements remaining in the solutions (especially for the Ag wires; this is unsurprising as they have not undergone chemical separation).

Several factors influence the choice of best Pd isotope ratio to use for mass bias corrections. For example, $^{110}Pd/^{106}Pd$ (note: $^{110}Pd$ was not measured here) has the same average atomic mass (108) as $^{109}Ag/^{107}Ag$, but it suffers from the potential for significant Cd isobaric interferences on both isotopes ($^{110}Cd$ = 12.49 %; $^{106}Pd$ = 1.25 %), which is a noteworthy consideration for unprocessed Ag samples. Additionally, trace amounts of Zr in solution have been recognised to have major effects on the measurement of Pd isotopes as Zr-oxide can cause molecular interferences with Pd (e.g. $^{90}Zr + ^{16}O \approx ^{106}Pd$) [42]. We do not observe a resolvable effect from this phenomenon in our dataset; $\varepsilon^{109}Ag$ values normalised with both $^{108}Pd/^{105}Pd$ and $^{106}Pd/^{105}Pd$ produce Ag isotope compositions within uncertainty of each other (Fig. 3). However, due to lower individual measurement precision and greater scatter in the dataset when using $^{106}Pd/^{105}Pd$ for mass bias corrections (See full dataset in ESI), $^{108}Pd/^{105}Pd$ is preferred given that it has a closer average atomic mass (106.5) to the ideal value (108).

### 3.2 Long term instrument stability

To monitor the long-term instrument stability of the Ag isotope measurements at Monash University, all measurements of the NIST SRM 978a Ag isotope standard in over 13 sessions over a 1-year period are compared in Figure S9. The mean Pd mass bias-corrected $^{109}Ag/^{107}Ag$ ratio measured at Monash University is 0.92566 ± 0.00006 (2 s.d.; n = 380).. This value compares favourably with previous studies, given that it is smaller than previously reported long term reproducibility's of $^{109}Ag/^{107}Ag$ ratios of 0.92603 ± 0.00009 [5] and 0.92669 ± 0.00025 [2]. The variability in the average $^{109}Ag/^{107}Ag$ ratio within a single analytical session ranged between± 0.000012 to 0.0.000043 (2 s.d.). Ultimately, this value is not particularly important for assessing the reproducibility of Ag isotope measurements of unknowns, given that all measurements are standard-sample bracketed. However, it is useful for evaluating the stability of the instrument during a specific interval. Analytical sessions with poor instrument stability (> ± 0.00003) often display poorer reproducibility of replicate analyses, as standard-sample measurements rely on good instrument stability with limited intra standard drift to be able to perform accurate mass bias corrections.

### 3.3 Internal precision, external reproducibility, and data accuracy

Individual measurement uncertainties (2 se) reported here vary between $\varepsilon^{109}Ag$ ± 0.11 and 0.26, and fluctuate over a relatively constant range independent of the nature of the sample (i.e. synthetic or natural). Furthermore, these uncertainties appear uncorrelated with the measured Ag signal intensity (Fig. 4), suggesting that the uncertainties are approaching the theoretical minimum analytical uncertainty currently achievable, based on counting statistics using conventional amplifiers (i.e. $10^{11}$ Ω) for this length of analysis. Instead, analysis precision appears a function of instrument stability at the time of measurement (i.e. it is controlled by the influence of interference or background corrections, matrix effects, or how well the mass bias of Pd follows that of Ag during different analyses). By comparing the propagated uncertainties for different sample types, it is possible to assess the effect of the chemical separation procedure on the precision of Ag isotope measurements. The average propagated measurement uncertainty for the pure synthetic in-house Ag standard 'Sigma MON' was $\varepsilon^{109}Ag$ ± 0.27 (n = 34) compared to $\varepsilon^{109}Ag$ ± 0.25 (n = 20) for the CEZAg Au standard, indicating that the chemical processing technique has no resolvable effect on the precision of the Ag isotope measurements.

At the beginning of each measurement session, the 'Sigma MON' Ag solution, was analysed several times, bracketed by NIST SRM 978a, and the offset between the two solutions was monitored to ensure that the instrument was performing satisfactorily. This 'Sigma MON' Ag solution has an average composition of $\varepsilon^{109}Ag = 1.32 \pm 0.31$ (2 s.d.; n = 34; Fig. 5) and provides an indication of the long-term instrument stability of the Ag isotope analyses herein. As a first test of the accuracy of the separation protocol implemented here, two synthetic Au-Ag standards Sigma5 and Sigma10 were processed through chemistry to purify the Ag and measured several times on the instrument. The average compositions of Sigma5 and Sigma10 are $\varepsilon^{109}Ag = 1.23 \pm 0.12$ (2 s.d.; n = 3; Table 2) and $\varepsilon^{109}Ag = 1.13 \pm 0.20$ (2 s.d.; n = 2), respectively, which are identical within analytical uncertainty to the average of the un-processed 'Sigma MON' Ag solution (Fig. 5). As the Ag component of the synthetic Au-Ag standards was comprised of the Ag solution, this result demonstrates the accuracy of the chemical separation and conversion process. These synthetic standards were only used for initial testing prior to the CEZAg standard being acquired. Additionally, the synthetic solutions do not represent a true matrix-matched proxy for real Au samples (i.e. they are lacking other common trace contaminants Cu, Pb etc.)[‡]. Therefore, the CEZAg Au standard is preferred to quantify the external reproducibility of the chemical processing and Ag isotope measurements herein. Six aliquots of the CEZAg standard were processed through chemistry and measured over the course of three analytical sessions. The mean of all individual measurements

View Article Online
DOI: 10.1039/D3JA00374D

of the CEZAg standard is $\varepsilon^{109}$Ag = 0.34 ± 0.18 (2 s.d.; n = 20), and the grand mean of the six processed aliquots is $\varepsilon^{109}$Ag = 0.34 ± 0.13 (2 s.d.; n = 6). This value is identical within analytical uncertainty to the previously reported determinations [5, 6] of the CEZAg standard (Table 2; Fig. 5), demonstrating that this chemical processing method produces accurate $\varepsilon^{109}$Ag measurements. Conservatively, the uncertainty on unknown Au samples processed using this technique is considered to be ≈ 0.20 ε.

### 3.4 Analysis of pure Ag materials

Four native Ag wire samples from the Elura Mine (Fig. 6a) were analysed without chemical processing to test the precision and accuracy of Ag isotope measurements of unprocessed high-purity Ag samples (Table 3). The native Ag samples have comparable, but slightly worse internal replicate reproducibility compared to the chemically processed CEZAg and Fosterville Au samples. This is likely due to the small amount of matrix elements present in the solution, which may contribute to instrument stability, or cause isobaric interferences. There is always a trade-off between these minor effects and the effort and risk associated with chemically processing samples. Any form of chemical processing of samples introduces some risk of contamination or artificial fractionation. Chugaev and Chernyshev (2012) found the typical purity of native Ag wires was > 97 wt.%, with the main matrix elements being Fe, Cu, Zn, Ni and Mg, and concluded that chemical processing was not required for native Ag samples of this purity. Argapadmi et al. (2018) also analysed native Ag ores mostly without chemical purification following screening for trace element contaminants, although one sample with an elevated Cu content required chemical purification. For large sample sets where the purity of the Ag is unknown, we advocate geochemical analysis to confirm the quantity and type of matrix elements (particular those which are known to cause isobaric interferences, e.g. Zn) should be conducted prior to MC-ICP-MS measurements to make the assessment as to whether chemical processing is required.

Each wire was analysed multiple times across two analytical sessions and the average reproducibility of repeat measurements was $\varepsilon^{109}$Ag = ± 0.24 (2 s.d.). The range in Ag isotope composition of the native Ag wires is $\varepsilon^{109}$Ag = -2.40 to -0.35 (2.05 ε), which is a very narrow range compared to the total range observed in previous native Ag measurements (ca. 30 ε; Mathur et al., 2018). However, the range of Ag isotope compositions of native Ag wires reported by previous studies is comparable to the range found in this study. Chugaev and Chernyshev (2012) found a range isotopic values of $\varepsilon^{109}$Ag from -0.9 to 1.9 (2.8 ε) in four native Ag wires, each from different countries. Mathur et al. (2018) analysed six native Ag wires from a single mesothermal deposit in Spain and found a similar range of $\varepsilon^{109}$Ag values from -2.57 to -0.95 (1.62 ε). Combining results from all measurements of native Ag wires gives an average isotopic composition of $\varepsilon^{109}$Ag = -0.88 ± 3.10 (2 s.d.; n = 14) and a range of 4.47 ε. This average is lighter, but within uncertainty of the estimated composition of bulk silicate Earth of $\varepsilon^{109}$Ag = 2.2 ± 0.7 (2 s.d.; n = 13; [19]). Native Ag samples from hypogene ore deposits range from $\varepsilon^{109}$Ag -3.71 to +4.29 (8.00 ε; n = 52; [1, 3]) similar to the Ag wires, however, supergene altered samples are significantly more variable with $\varepsilon^{109}$Ag ranging -8.64 to 21.42 (30.06 ε; n = 26; [3]), suggesting significant Ag isotope fractionation in low temperature fluids.

### 3.5 Analysis of natural Au nuggets

Silver isotope compositions have been obtained from 7 separate Au nuggets from 4 discrete samples from the Fosterville Gold Mine in Victoria, Australia (Fig. 6b). Samples were analysed at both Monash University using the conversion process for Au samples described herein and a more conventional 2 column methodology [5] at the CEZ to validate the accuracy of Ag isotope measurements generated using the ammonia-ascorbic acid conversion process (Table 3). Replicate analyses of individual Au nuggets at Monash University are extremely consistent with an average reproducibility of $\varepsilon^{109}$Ag = ± 0.19 (2 s.d.). Furthermore, there is excellent agreement between the Ag isotope data generated using both methodologies, with the Monash and CEZ results within analytical uncertainty of each other in all bar one instance (Fig. 6b). However, this discrepancy remains relatively small (max $\Delta^{109}\mathrm{Ag}_{\mathrm{MON\text{-}CEZ}}$ = 0.52) to the overall spread in the Fosterville Au (see below), furthermore, this is not unexpected given each analyses represents the dissolution of a different Au fragment, which may possess natural Ag isotope heterogeneities. The excellent agreement between Ag isotope data generated using two distinct separation protocols provides further confirmation of the accuracy of the new methodology reported here.

The overall range of the Fosterville Au samples is only $\varepsilon^{109}$Ag = 3.91 to 5.91 (2.00 ε), which is relatively restricted compared to the range seen in Au samples globally (ca. 16.0 ε; [1, 5, 6]). The Fosterville Au samples do nevertheless demonstrate that statistically resolvable Ag isotope variation can occur within a single Au deposit, a phenomenon also observed at the Sheba deposit, South Africa [1]. Even when considered on the regional scale, the Fosterville samples show significantly less variability than observed across the Victorian Gold Field [6] where $\varepsilon^{109}$Ag ranges from -8.3 to 6.6 (14.9 ε). Interestingly, average Fosterville Au has $\varepsilon^{109}$Ag = 4.89 ± 1.70 (2 s.d.; n = 7), which is marginally isotopically heavier than Au from Bendigo 27 km to the west, in comparable rock sequences; cf. [43], the only other location with a comparable amount of data, which has $\varepsilon^{109}$Ag = 3.07 ± 1.08 (2 s.d.; n = 6). Although beyond the scope of this study, understanding the physio-chemical conditions responsible for the Ag isotope discrepancy between these two closely spaced ore deposits hosted with the same geological units and presumably sourced from comparable basement derived fluids units would be worthy of further investigation.

## Conclusions

We have presented a comprehensive description of a novel processing technique to enable fast and accurate Ag isotope measurements of native Au samples. This method uses a single ion exchange column for removal of matrix elements, followed by a chemical conversion of Ag from chloride to nitrate form using ammonium hydroxide and ascorbic acid. This approach is not only simpler and faster than previous methods, it also eliminates the risk of Ag loss during chloride to nitrate conversion. Multiple analysis of the CEZAg Au standard returned a mean $\varepsilon^{109}$Ag = 0.34 ± 0.13, which is within analytical uncertainty of previously reported values. Additionally, natural Au gold nuggets from the Fosterville Au mine analysed using the chemical conversion process described herein at Monash University, Australia and a multiple column method [5] processed at the CEZ, Germany, produced Ag isotope compositions within analytical uncertainty, further confirming the accuracy of the measurements generated using this new method. The external reproducibility of the protocol described herein ($\varepsilon^{109}$Ag ± ca. 0.20) is also comparable with previous studies, demonstrating that this new method can achieve accurate and precise Ag isotope measurements of native Au samples.

## Author Contributions

**Alex McCoy-West**: Writing - Original Draft; Validation; Visualization, Supervision; Methodology. **Alison Davis**: Methodology; Investigation; Conceptualisation; Writing - Original Draft; Visualization; **Ashlea Wainwright**: Investigation; Writing - Review & Editing; Supervision; **Andrew Tomkins**: Writing - Review & Editing; Supervision; Funding acquisition.

## Conflicts of interest

There are no conflicts to declare.

## Acknowledgements

We are very gratefully to Michael Brauns and Gerhard Brügmann for undertaking comparative Ag isotope analyses at CEZ, Manheim. AMW acknowledges ARC grants FL160100168 and DE210101395. AMD acknowledges receipt of an Australian Postgraduate Award PhD scholarship. AGT acknowledges ARC grant LP015100717. ANW acknowledges ARC grant FL160100168. Simon Hitchman, Wess Edgar, Nathan Phillips from Fosterville gold mine, then operated by Kirkland Lake Gold, are thanked for their assistance in obtaining gold samples. Tom Kapitany is thanked for providing native Ag samples. Massimo Raveggi, Yona Jacobson, and Oliver Nebel are thanked for technical assistance and discussions at Monash. We thank two anonymous journal reviewers for their constructive comments.

## Notes and references

‡ An additional consideration with the synthetic Au-Ag solutions is that a small amount of insoluble AgCl powder may form in the mixtures when the two primary solutions are combined, as the Sigma-Aldrich 1000 µg/mL Au solution used is dissolved in 5% HCl. This phenomenon potentially explains the marginally lighter composition of the Sigma10 replicates observed herein.

1. W. Argapadmi, E. R. Toth, M. A. Fehr, M. Schönbächler and C. A. Heinrich, *Economic Geology*, 2018, **113**, 1553-1570.
2. M. Schönbächler, R. W. Carlson, M. F. Horan, T. D. Mock and E. H. Hauri, *International Journal of Mass Spectrometry*, 2007, **261**, 183-191.
3. R. Mathur, A. Arribas, P. Megaw, M. Wilson, S. Stroup, D. Meyer-Arrivillaga and I. Arribas, *Geochimica et Cosmochimica Acta*, 2018, **224**, 313-326.
4. T. Fujii and F. Albarede, *Geochimica et Cosmochimica Acta*, 2018, **234**, 37-49.
5. G. Brügmann, M. Brauns and R. Maas, *Chemical Geology*, 2019, **516**, 59-67.
6. C. R. Voisey, R. Maas, A. G. Tomkins, M. Brauns and G. Brügmann, *Economic Geology*, 2019, **114**, 233-242.
7. M. Schönbächler, R. W. Carlson, M. F. Horan, T. D. Mock and E. H. Hauri, *Geochimica et Cosmochimica Acta*, 2008, **72**, 5330-5341.
8. F. Albarède, J. Blichert-Toft, M. Rivoal and P. Telouk, *Geochemical Perspectives Letters*, 2016, **2**, 127-137.
9. J. Milot, J. Blichert-Toft, M. A. Sanz, C. Malod-Dognin, P. Télouk and F. Albarède, *Geology*, 2021, **50**, 422-426.
10. J. Milot, C. Malod-Dognin, J. Blichert-Toft, P. Télouk and F. Albarède, *Chemical Geology*, 2021, **564**, 120028.
11. M. Vaxevanopoulos, G. Davis, J. Milot, J. Blichert-Toft, C. Malod-Dognin and F. Albarède, *Journal of Archaeological Science*, 2022, **145**, 105645.
12. M. Kałaska, R. Mathur, G. Kamenov, J. Chyla, P. Prządka-Giersz and M. Giersz, *Archaeometry*, 2022, **64**, 1168-1186.
13. A.-M. Desaulty, P. Telouk, E. Albalat and F. Albarède, *Proceedings of the National Academy of Sciences*, 2011, **108**, 9002-9007.
14. Y. Luo, E. Dabek-Zlotorzynska, V. Celo, D. C. G. Muir and L. Yang, *Analytical Chemistry*, 2010, **82**, 3922-3928.
15. L. Yang, E. Dabek-Zlotorzynska and V. Celo, *Journal of Analytical Atomic Spectrometry*, 2009, **24**, 1564-1569.
16. J. H. Chen and G. J. Wasserburg, *Geochimica et Cosmochimica Acta*, 1983, **47**, 1725-1737.
17. V. R. Murthy, *Physical Review Letters*, 1960, **5**, 539-541.
18. K. F. Flynn and L. E. Glendenin, *Physical Review*, 1969, **185**, 1591-1593.
19. M. Schönbächler, R. W. Carlson, M. F. Horan, T. D. Mock and E. H. Hauri, *Science*, 2010, **328**, 884-887.
20. R. W. Carlson and E. H. Hauri, *Geochimica et Cosmochimica Acta*, 2001, **65**, 1839-1848.
21. S. J. Woodland, M. Rehkämper, A. N. Halliday, D. C. Lee, B. Hattendorf and D. Günther, *Geochimica et Cosmochimica Acta*, 2005, **69**, 2153-2163.
22. H. Hamaguchi and R. Kuroda, *Geochimica et Cosmochimica Acta*, 1959, **17**, 44-52.
23. N. Braukmüller, F. Wombacher, A. Bragagni and C. Münker, *Geostandards and Geoanalytical Research*, 2020, **44**, 733-752.
24. Z. Wang, H. Becker and F. Wombacher, *Geostandards and Geoanalytical Research*, 2015, **39**, 185-208.
25. G. A. Palyanova, *Geology of Ore Deposits*, 2020, **62**, 383-406.
26. H. A. Cocker, J. L. Mauk and S. D. Rabone, *Mineralium Deposita*, 2013, **48**, 249-266.
27. G. W. Morrison, W. J. Rose and S. Jaireth, *Ore Geology Reviews*, 1991, **6**, 333-364.
28. A. V. Chugaev and I. V. Chernyshev, *Geochemistry International*, 2012, **50**, 899-910.

View Article Online
DOI: 10.1039/D3JA00374D

29. D. Wang, R. Mathur, Y. Zheng, H. Wu, Y. Lv, G. Zhang, R. Huan, M. Yu and Y. Li, *Mineralium Deposita*, 2022, **57**, 701-724.
30. J.-L. Wang, H.-Z. Wei, A. E. Williams-Jones, G. Dong, Y.-F. Zhu, S.-Y. Jiang, J. Ma, S. V. Hohl, X. Liu, Y.-C. Li and J.-J. Lu, *Geochimica et Cosmochimica Acta*, 2022, **322**, 24-42.
31. A. Arribas, R. Mathur, P. Megaw and I. Arribas, *Geochemistry, Geophysics, Geosystems*, 2020, **21**, e2020GC009097.
32. J. L. White, R. L. Orr and R. Hultgren, *Acta Metallurgica*, 1957, **5**, 747-760.
33. C. H. Gammons and A. E. Williams-Jones, *Economic Geology*, 1995, **90**, 420-432.
34. J. I. Drever, *The geochemistry of natural waters*, Prentice hall Englewood Cliffs, 1988.
35. W. Songping and M. Shuyuan, *Materials Chemistry and Physics*, 2005, **89**, 423-427.
36. G. Guo, W. Gan, J. Luo, F. Xiang, J. Zhang, H. Zhou and H. Liu, *Applied Surface Science*, 2010, **256**, 6683-6687.
37. C. A. Perman, *Talanta*, 1979, **26**, 603-604.
38. C. N. Maréchal, P. Télouk and F. Albarède, *Chemical Geology*, 1999, **156**, 251-273.
39. A. J. McCoy-West, J. Godfrey Fitton, M.-L. Pons, E. C. Inglis and H. M. Williams, *Geochimica et Cosmochimica Acta*, 2018, **238**, 542-562.
40. T. E. Waight, J. A. Baker and D. Peate, *International Journal of Mass Spectrometry*, 2002, **221**, 229-244.
41. N. Dauphas, A. Pourmand and F.-Z. Teng, *Chemical Geology*, 2009, **267**, 175-184.
42. M. Ek, A. C. Hunt and M. Schönbächler, *Journal of Analytical Atomic Spectrometry*, 2017, **32**, 647-656.
43. C. R. Voisey, A. G. Tomkins and Y. Xing, *Economic Geology*, 2020, **115**, 1645-1664.

View Article Online
DOI: 10.1039/D3JA00374D

## Figures

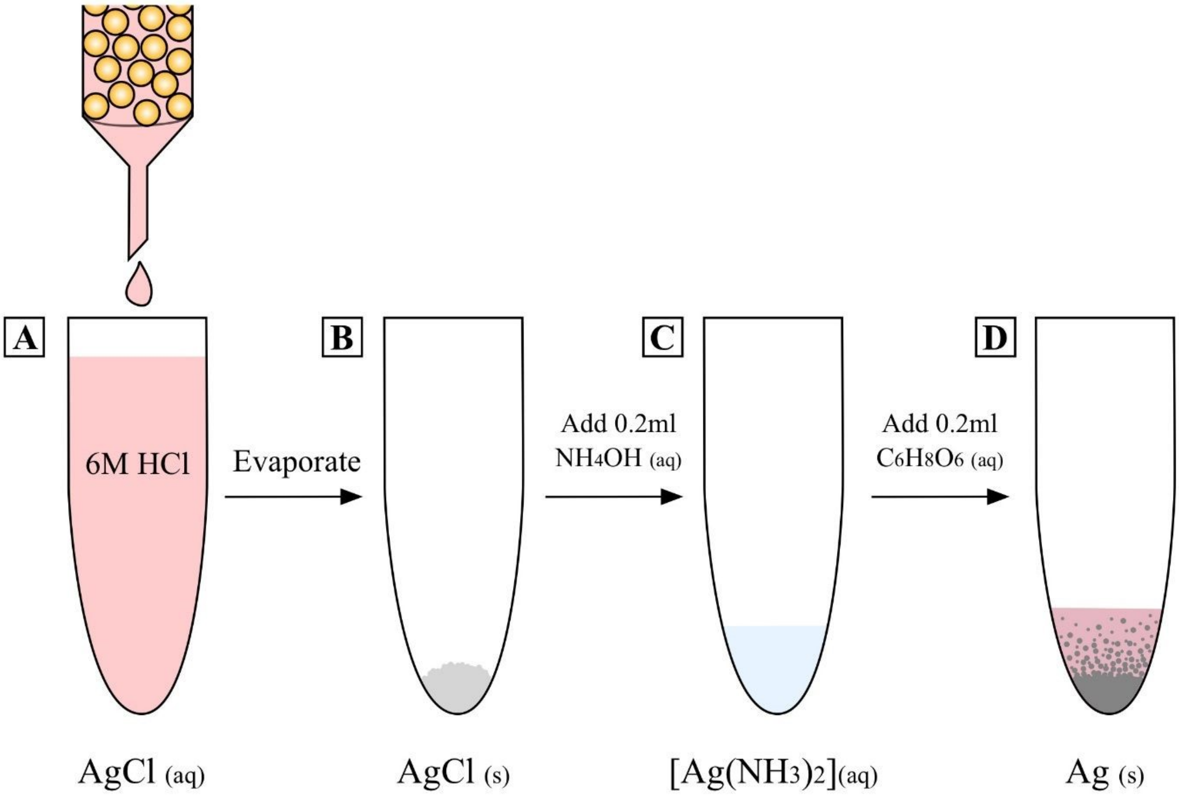

**Figure 1:** Schematic diagram illustrating the chemical conversion of Ag from chloride to nitrate form in preparation for mass spectrometry. (a) Collection of the Ag fraction following ion exchange chromatography. Yellow beads represent the resin bed of the column. (b) Following evaporation AgCl particles are formed. (c) The addition of ammonium hydroxide completely dissolves the Ag. (d) Pure Ag particles are precipitated following the addition of ascorbic acid.

View Article Online
DOI: 10.1039/D3JA00374D

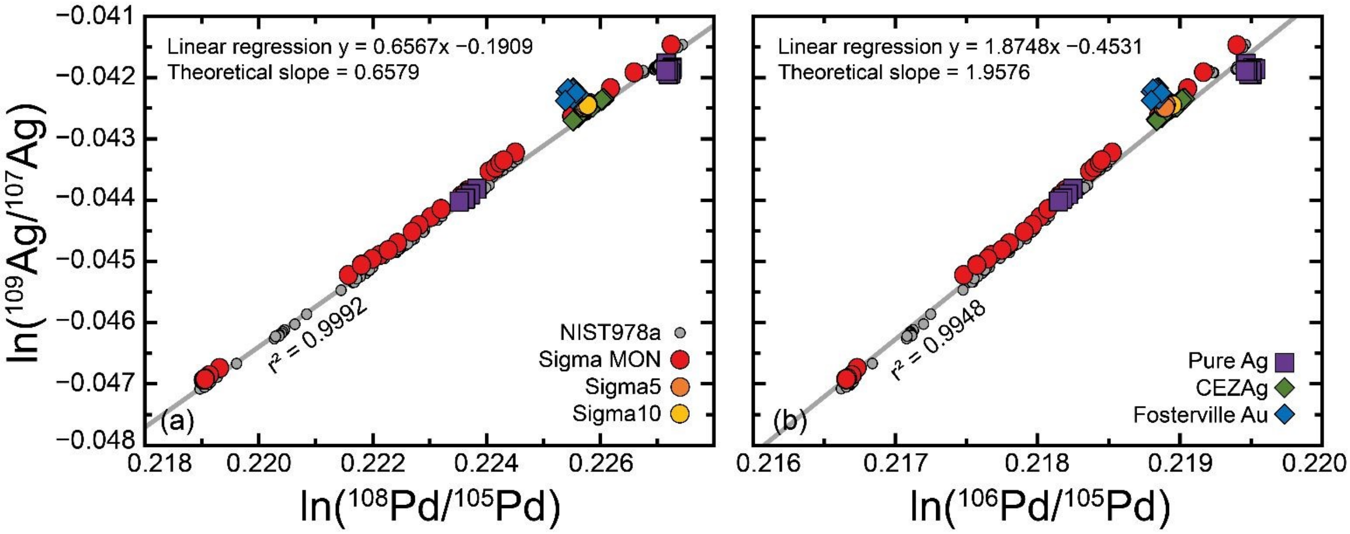

**Figure 2:** Natural logarithms of raw Ag and Pd isotope ratios. Linear regression is derived from bracketing standard NIST SRM978a. The unknowns, which have and have not undergone chemical separation, fall on very similar linear trends, indicating a lack of differential mass bias caused by interferences (i.e. isobaric or molecular) in the solutions. Theoretical slopes are predicted with exponential law equations $\frac{\ln\left(\frac{M_{^{109}\mathrm{Ag}}}{M_{^{107}\mathrm{Ag}}}\right)}{\ln\left(\frac{M_{^{108}\mathrm{Pd}}}{M_{^{105}\mathrm{Pd}}}\right)}$ and $\frac{\ln\left(\frac{M_{^{109}\mathrm{Ag}}}{M_{^{107}\mathrm{Ag}}}\right)}{\ln\left(\frac{M_{^{108}\mathrm{Pd}}}{M_{^{105}\mathrm{Pd}}}\right)}$.

View Article Online
DOI: 10.1039/D3JA00374D

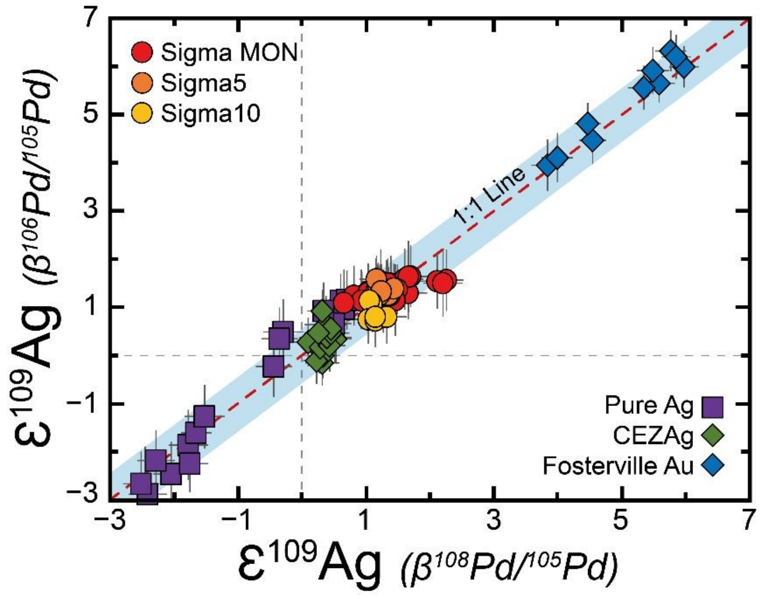

**Figure 3:** Plot comparing $\varepsilon^{109}$Ag mass bias corrected using both $^{108}$Pd/$^{105}$Pd and $^{106}$Pd/$^{105}$Pd for samples measured in this study. Shaded field around the 1:1 line represents an uncertainty of ± 0.055, the average uncertainty on $\varepsilon^{109}$Ag calculated using $^{106}$Pd/$^{105}$Pd normalisation herein. All analyses fall within uncertainty of the 1:1 line, confirming that data normalisation does not affect accuracy of Ag isotope ratios.

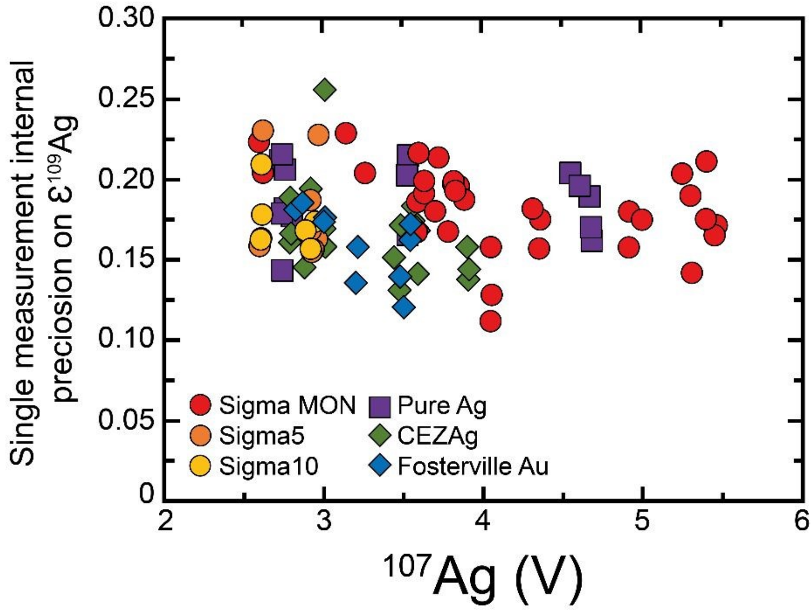

**Figure 4:** Plot comparing internal precision on $\varepsilon^{109}$Ag for all individual measurements included in this study (n = 96) relative to the average signal intensity of $^{107}$Ag. Increasing the signal intensity does not systematically result in more precise data, suggesting measurements are approaching the minimum theoretical uncertainty achievable based on counting statistics for this duration of analysis (45 cycles of 4 s integrations).

View Article Online
DOI: 10.1039/D3JA00374D

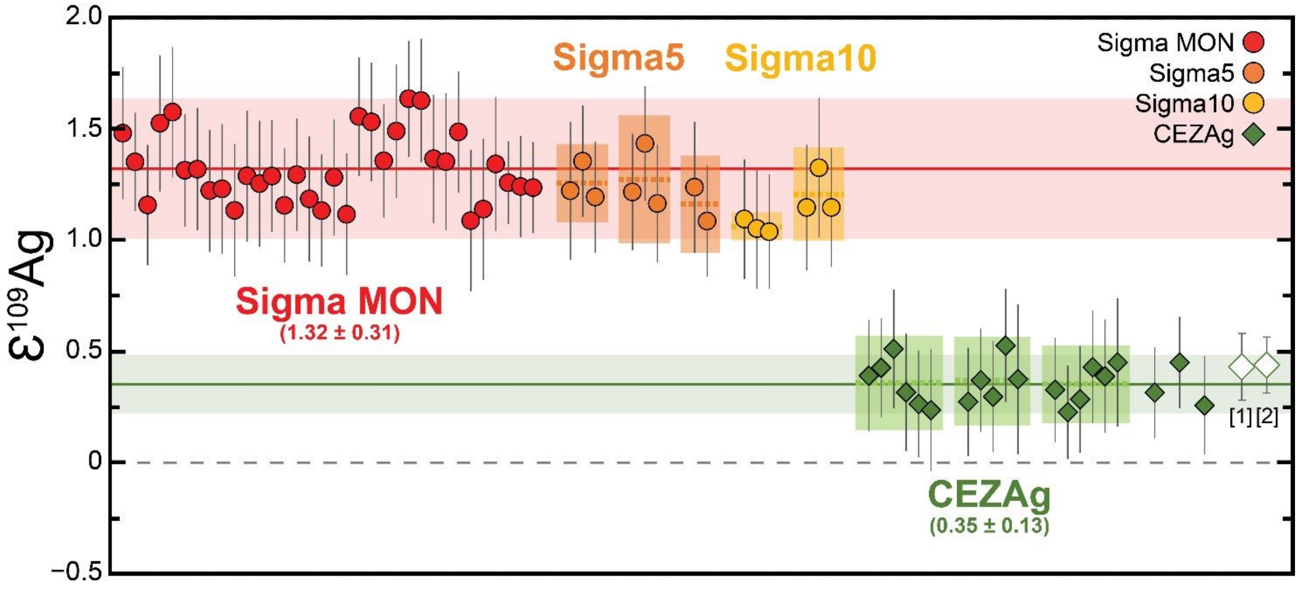

**Figure 5:** Long-term reproducibility of $\varepsilon^{109}$Ag of reference materials analysed in this study. The in-house Sigma MON solution was measured without chemical purification. Sigma5 and Sigma10 are synthetic Au-Ag mixtures, made from the same Sigma MON Ag solution, that have been chemically purified to isolate Ag. The CEZAg standard is made from dissolved natural Au nuggets, that were chemically purified. Each data point represents a single analysis, with error bars representing propagated 2 standard errors. Shaded fields with solid line represent long-term averages of Sigma ICP and CEZAg, with the shaded field representing 2 standard deviations. Shaded boxes with dotted lines represent the average composition ± 2 standard deviations of replicate measurements of the same digestion. Average compositions of previously published CEZAg data (hollow symbols) are taken from [1][5] and [2][6].

View Article Online
DOI: 10.1039/D3JA00374D

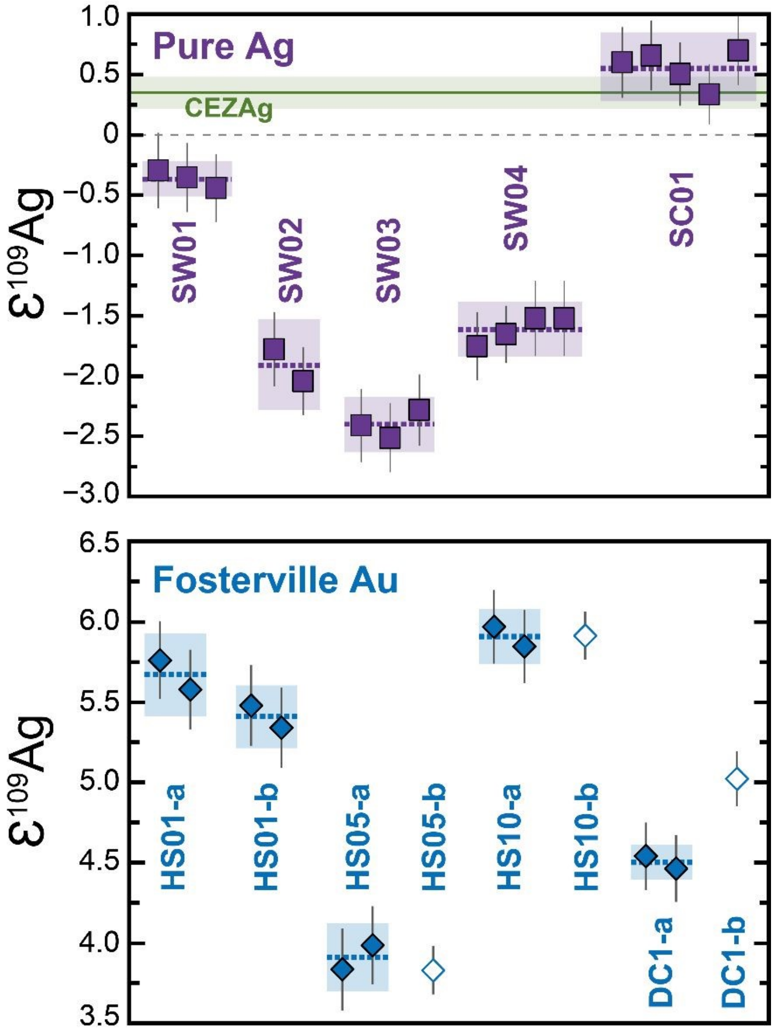

**Figure 6:** Reproducibility of $\varepsilon^{109}$Ag for the natural metallic Ag wires (a) and Fosterville Au (b) samples. Each data point represents a single analysis, with error bars representing propagated 2 standard errors. Shaded boxes with dotted lines represent the average composition ± 2 standard deviations of replicate measurements of the same digestion. (a) Metallic Ag samples were measured without chemical purification. The solid line represents the average composition of CEZAg herein, with the shaded field being 2 standard deviations. (b) Fosterville Au samples underwent chemical purification and Ag nitrate conversion as described herein. Hollow symbols represent comparative analyses of different Au nuggets separated from the same samples conducted at Curt-Engelhorn-Zentrum (CEZ) using a multiple column method.

View Article Online
DOI: 10.1039/D3JA00374D

## Tables

**Table 1:** Summary of the ion exchange procedure for Ag purification on the AG1-X8 column

| Volume | Eluent | Separation step |
|---|---|---|
| 3 x 1 ml<br>*(total 3 ml)* | 6 M HCl | Resin cleaning and pre-conditioning |
| 1 ml | 6 M HCl | Load sample, begin collecting Ag immediately |
| 8 x 0.5 ml<br>*(total 4 ml)* | 6 M HCl | Continue collecting Ag |

View Article Online
DOI: 10.1039/D3JA00374D

**Table 2:** Silver isotope measurements of reference materials

| Sample | $\varepsilon^{109}Ag$ | 2 SD | n |
|---|---|---|---|
| Sigma MON | 1.32 | 0.31 | 34 |
| Sigma5 | | | |
| Sigma5-1 | 1.26 | 0.17 | 3 |
| Sigma5-2 | 1.27 | 0.29 | 3 |
| Sigma5-3 | 1.16 | 0.21 | 2 |
| Mean | 1.23 | 0.12 | 3 |
| Sigma10 | | | |
| Sigma10-1 | 1.06 | 0.06 | 3 |
| Sigma10-2 | 1.21 | 0.21 | 3 |
| Mean | 1.13 | 0.20 | 2 |
| CEZAg | | | |
| CEZAG-1 | 0.36 | 0.21 | 6 |
| CEZAG-2 | 0.37 | 0.20 | 5 |
| CEZAG-3 | 0.35 | 0.17 | 6 |
| CEZAG-4^ | 0.31 | 0.20 | *1* |
| CEZAG-5^ | 0.45 | 0.21 | *1* |
| CEZAG-6^ | 0.26 | 0.22 | *1* |
| Mean | 0.342 | 0.127 | 6 |
| Brugmann | 0.43 | 0.15 | 18 |
| Voisey | 0.438 | 0.126 | 7 |

Sigma MON was measured unprocessed. Synthetic Au-Ag solutions Sigma5 and Sigma10 and natural Au standard CEZAg were measured following chemical purification. ^Analyses that consist of only 1 replicate on the mass spectrometer are reported with propagated 2 se uncertainties. Data is present relative NIST SRM 978a.

View Article Online
DOI: 10.1039/D3JA00374D

**Table 3:** Silver isotope and concentration measurements of metallic Ag and Fosterville Au samples

| Sample | Weight (mg) | Ag (%) | Cu (µg/g) | $^{107}$Ag (V) | $\varepsilon^{109}$Ag | 2SD | n |
|---|---|---|---|---|---|---|---|
| **Metallic Ag** | | | | | | | |
| SC01 | | 100 | | 4.63 | 0.56 | 0.29 | 5 |
| SW01 | 1.05 | 100 | | 3.53 | -0.36 | 0.15 | 3 |
| SW02 | 9.49 | 100 | | 2.78 | -1.39 | 0.37 | 2 |
| SW03 | 4.77 | 100 | | 2.74 | -2.40 | 0.23 | 3 |
| SW04 | 5.23 | 100 | | 2.74 | -1.61 | 0.23 | 4 |
| **Fosterville Au** | | | | | | | |
| HS01-a | 14.74 | 5.77 | 192 | 3.54 | 5.67 | 0.26 | 2 |
| HS01-b | 2.43 | 6.23 | 1579 | 3.01 | 5.41 | 0.19 | 2 |
| HS05-a | 1.96 | 8.67 | 198 | 2.85 | 3.91 | 0.21 | 2 |
| HS05-b* | | | | | 3.83 | 0.15 | |
| HS10-a | 13.2 | 5.48 | 322 | 3.21 | 5.90 | 0.17 | 2 |
| HS10-b* | | | | | 5.91 | 0.15 | |
| DC01-a | 19.24 | 5.44 | 205 | 3.49 | 4.50 | 0.11 | 2 |
| DC01-b* | | | | | 5.02 | 0.17 | |

Letters (a,b) refer to a separate dissolution of a different gold nuggets from different areas of the same hand sample. *Comparative analyses conducted at CEZ, Manheim, Germany. n = number of replicates comprising a measurement. Pd was below the detection limit in all samples. Data is present relative NIST SRM 978a.